GEOSCIENCES 2006

“Baby-granites” in migmatites from Chepinska river valley, Western Rhodope – geochemistry and U-Pb isotope dating on monazite and zircon

Zlatka Cherneva[1,2], Maria Ovtcharova[3], Dimo Dimov[1], Albrecht von Quadt[4]

[1] Sofia University “St. Kl. Ohridski”, 15 Tzar Osvoboditel blvd., 1504 Sofia; E-mail: cherneva@gea.uni-sofia.bg
[2] Geological Institute, BAS, 1113 Sofia
[3] Geneva University, rue des Maraochers 13, CH-1205 Genève; E-mail: Maria.Ovtcharova@terre.unige.ch
[4] IGMR, ETH Zurich, Clausiusstr. 25,8092 Zurich; E-mail: quadt@erdw.ethz.ch

Key words: migmatization, U-Pb isotope, monazite, zircon, Western Rhodope

The Eocene — Oligocene migmatization in the Central Rhodope is well known long since U-Pb isotope dating of monazite and zircon produced incontestable results. The migmatite age variation 36 to ~50 Ma is structurally dependent (Ovtcharova et al., 2002; Cherneva et al., 2003) supporting the idea of later exhumation of a diatexite dome core structure (Central Rhodopian Dome, Ivanov et al., 2000). The time span of synmetamorphic generation and in situ crystallization of crustal anatectic melts in the Central Rhodope overlaps partially the period of intrusive granite magmatism in the Western Rhodope (Upper Cretaceous — Eocene, 68 Ma, 43—40 Ma, and 37.5 Ma; Peytcheva et al., 1998; von Quadt, Peycheva, 2005). Part of the host rocks there are migmatites of unknown age, described as “granitized” rocks (Valkov et al., 1989).

Geological setting and field relations

Migmatites are widespread to the north-east of the Rila-Rhodope batholith. Migmatitic gneisses of metadioritic to metagranodioritic compositions form a domain, situated just below the North Rhodopian thrust (Geological map of Bulgaria, scale 1:200 000; Ivanov et al., 1989; Gerdjikov et al., this volume). The foliation dips to NE, N and NW; and the mineral lineation and syn-migmatitic fold hinges display a NW-SE trend in the range of 310—340°. The mesoscopic shear-sense criteria confirm the SE direction of tectonic transport.

The field observations cover outcrops along the Chepinska, Mutnitsa, and Stara river valleys, 12—15 km far of the Rila-Rhodope batholith contact. The migmatites are dominated by concordant to the foliation leucosomes that show subsolidus ductile deformation. Domains of lower deformation preserved metric scale irregular to lens-shaped granite bodies (fig. 1). These display distinct nevertheless gradational contacts with the adjacent migmatitic gneisses. The textures are inhomogeneous, massive or nebulitic, due to visible gneissic relics. At some places massive domains of gravitational melt migration broke the foliation in the gneiss matrix (anatectic erosion of mesosome). Based on migmatitic structures and morphology in the area we use the term “baby-granites” and consider these bodies as small anatectic melt portions separated at the end of the regional ductile deformation.

Numerous cross-cutting veins (granitic, aplitic and pegmatitic) penetrate the migmatites and display diffusive to sharp intrusive contacts. The relationships between cross-cutting veins and migmatites suggest syn- to post migmatization intrusion of the allochtonous granite magma, related most prob-

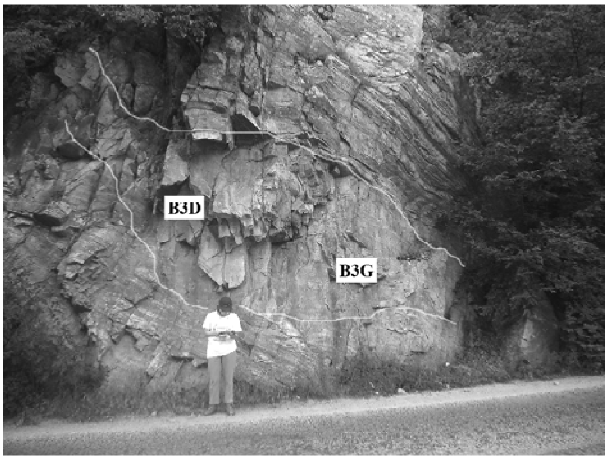

Fig. 1. Anatectic granite body NNE from Cepina railway station (GPS point: N 42.10642; E 024.10586)

ably to the younger granite units (Unit 2 and 3, Kamenov et al., 1999) of the Rila-Rhodope Batholith (RRB).

Samples studied

The study focuses attention on the outcrops near to the Cepina railway station in the Chepinska river valley. The selected samples represent: migmatitic gneisses of dioritic composition (B38G) and leucosome saturated biotite gneisses (B3A, B39G); concordant leucosomes formed in situ (B3B, B39L), and injected parallel to the foliation (B38L); anatectic "baby" granites from two separate bodies B3D and B3G (fig. 1), and B37. The rock-forming mineral assemblages comprise biotite, plagioclase, K-feldspar and quartz, with amphibole in the dioritic gneisses. The products of migmatization are quartz-feldspar dominated, with variable mineral proportions on a thin-section scale. Missing peritectic mafic minerals suggest water-saturated melting. The accessory mineral assemblages in the gneisses include magnetite, zircon, allanite, apatite, and titanite. The concordant leucosomes contain sparse zircon grains only, except for B38L, where abundant zircon and allanite are present. Monazite appears in the anatectic granites. It is found in mineral separates, together with allanite, apatite, zircon and magnetite.

Geochemistry

The rocks are metaluminous to slightly peraluminous (gneisses A/CNK 0.7—1.1, leucosomes and anatectic granites 0.9—1.2). The normative mineral proportions of the later correspond to low-temperature granite melts. The major elements variation of the gneisses is strongly affected by the presence of a melt, nevertheless dominant occurrence of Ca-alkaline magmatic protoliths could be assumed. The LIL elements distributions change systematically in the succession gneisses → in situ formed leucosomes → anatectic granite bodies. Increasing K/Ba, and Rb/Sr, and decreasing Ba/Rb ratios mark trends consistent with differentiation of felsic magma. They emphasize the role of the most incompatible LILE during anatectic melt migration and crystallization. The lower contents of HFSE (Zr, Y, Th, U) and REE in the products of migmatization suggest limited solubility of accessory phases in the melt. The contents of Zr and LREE (fig. 2a) however cluster close to the saturation concentrations in felsic peraluminous melts at 700—750°C (Watson Harrison, 1983; Watt, Harley, 1993). The temperatures would theoretically be high enough to cause advanced melting at water-saturated conditions, involving most mafic minerals and producing melts enriched in Fe, Mg and Ca, which is not observed. The εHf values of the dated zircons (0.3 to 4.7, fig. 3a) support an idea of zircon inheritance from orthometamorphic rocks of mixed crustal-mantle origin.

The REE patterns and relationships with LILE and HFSE display features typical for amphibolite facies water-saturated melting (low REE melts with a positive Eu-anomaly) that appear from in situ leucosome and anatectic granite compositions (fig. 2 b, c, e, f). Very close characteristics have the anatectic granite melts in the Central Rhodope (Cherneva, Georgieva, 2005). The variation of the Eu/Eu* values of anatectic granite bodies (fig. 3f), and the positive correlation with K/Rb (fig. 2 3c) could reflect contamination with gneiss relics (biotite) resulting

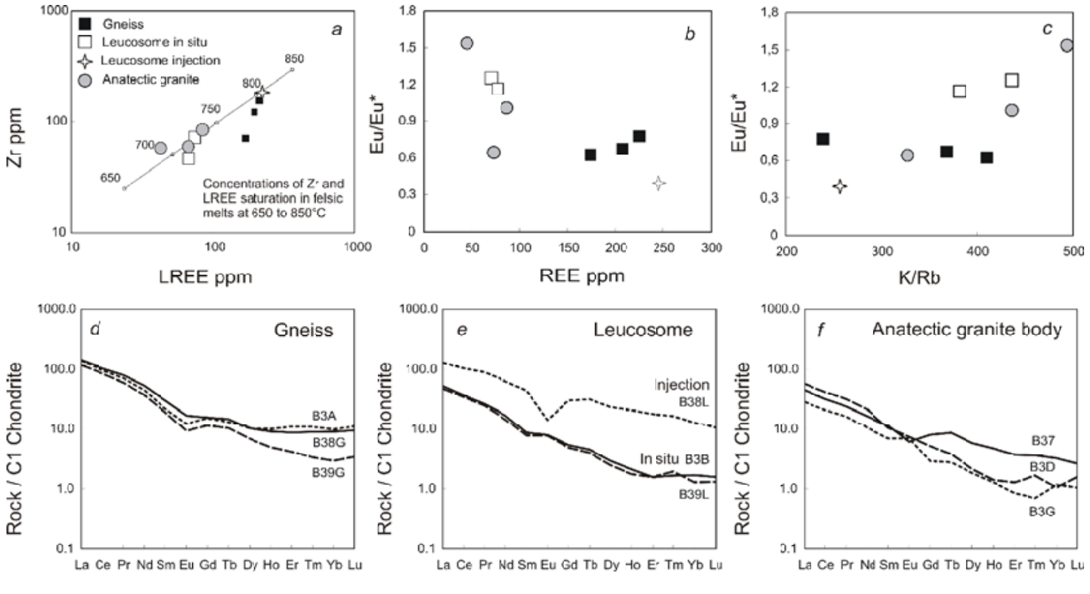

Fig. 2. Geochemical data on the migmatites from the Chepinska river valley. See the text for details

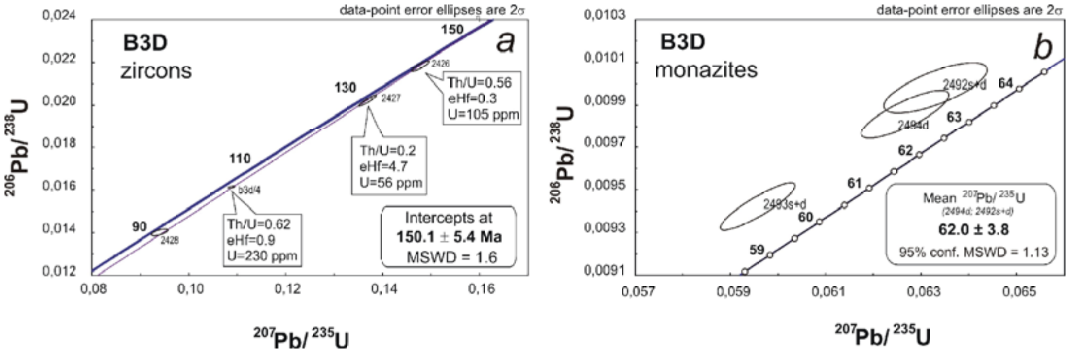

Fig. 3. Concordia plots showing U-Pb TIMS dating of a) single-zircons, and b) single monazites

in local inhomogeneity of the melt. The injected leucosome differs from in situ formed ones by higher HFSE and REE, low La/Yb ratio, and deep negative Europium anomaly (fig. 2a, b, c, e) resembling a strongly differentiated felsic granite magma. Similar distribution patterns display Unit 3 granites of the RRB (Kamenov et al., 1999).

U-Pb geochronological method and results

Zircons and monazites from sample B3D were dated by ID-TIMS (Isotope Dilution-Thermal Ionisation Mass Spectrometry) U-Pb techniques on single grains. In order to minimize the effects of secondary lead loss the zircons were air abraded prior to analysis while the monazites were not pretreated. Single zircons were selected, weighed and loaded for dissolution into pre-cleaned miniaturized Teflon vessels. After adding a mixed ^{205}Pb-^{235}U spike zircons were dissolved in HF + 7N HNO_3 and monazites in 6N HCl. Pb and U were separated by anion exchange chromatography in 40 μl micro-columns, using minimal amounts of ultra-pure HCl. The isotopic analyses were performed at ETH-Zurich on a MAT262 mass spectrometer equipped with an ETP electron multiplier backed by a digital ion counting system. The multiplier was calibrated by repeated analyses of the NBS 982 standard (Todt et al., 1996). Mass fractionation effects were corrected for 0.09±0.05 per a.m.u. Both lead and uranium were loaded with 1ml of silica gel-phosphoric acid mixture on outgassed single Re-filaments, and isotope ratios determined by sequential measurement of all ion beams on the electron multiplier. Total procedural common Pb concentrations were 0.8pg for zircon and monazite. The uncertainties of the spike and blank lead isotopic composition, mass fractionation correction, and tracer calibration were taken into account and propagated to the final uncertainties of isotopic ratios and ages. Calculation of ages and averages was done with the Isoplot/Ex v. 3 program of Ludwig (2005). Ellipses of concordia diagrams represent 2 sigma uncertainties.

Four long prismatic zircons were selected and analyzed, all of them showing different degree of Pb loss. All analysis are straddling a discordia line, which anchored through zero yields an upper intercept age of 150+/-5 Ma (MSWD 1.6), fig. 3a. Having in mind the low saturation temperature for zircons in anatectic melts (fig. 3a) we assume inheritance of these zircons from the substratum, accompanied with a certain degree of Pb loss, and therefore we interpret the upper intercept to reflect the Zr crystallization in the former magmatic protolith. Due to intensive air abrasion the possible overgrowth resulted from migmatitic melt crystallization was probably partly removed. When the discordia line is not anchored to zero the lower intercept is 37+/-27 Ma and upper intercept is 162+/-13 Ma. Three single monazite grains were analyzed from the same sample. The data are all inversely discordant due to ^{230}Th excess and their ^{207}Pb/^{235}U age varies between 59 Ma and 63 Ma (fig. 3b). The age variation is interpreted to be due to inhomogeneous mixture of different age components in Mnz (probably old core and younger rim). No definitive conclusion on the time of the monazite crystallization can be drawn from these data; we envisage a complex growth history of monazite, partly linked to migmatitic melt crystallization and therefore the time of “baby-granite” formation. The scattering U-Pb TIMS ages of single monazite grains are indication for younger overgrowth on old cores which can not be resolved without in-situ isotopic dating.

Conclusions

The main features of migmatites studied could be summarized as follows: 1) small anatectic melt portions, produced by amphibolite facies water-saturated melting; 2) limited participation of mafic minerals in the process of melting; 3) possible inheritance of accessory minerals from the substratum; 4) melt separation at the end of the regional ductile deformation; 5) syn- to post migmatization intrusion of allochtonous granite magma belonging most probably to the younger units of the RRB. The 150 Ma old zircon in the anatectic granite body B3D was inherited most probably from a magmatic protolith of mixed crustal-mantle origin. The best candidates are widespread gneisses of metadioritic composition. The time span of the melting event is supposed to be closer to the late RRB magmatic activity (43—37 Ma), than to the obtained monazite age of 59—63 Ma. The exact timing of monazite formation itself needs further detailed study.

Acknowledgements. The National Science Fund of the Ministry of Education and Science in Bulgaria supported part of this study financially, grant SSRAU-ES-05/2005.

References

Cherneva, Z., M. Ovtcharova, S. Arkadakskiy, A. von Quadt, I. Peytcheva. 2003. Accessory minerals behaviour during Eocene melting of Hercynian granitoids in the Central Rhodopian Dome, Bulgaria. — *Final GEODE-ABCD Workshop, Seggauberg, Austria*, 25—26.

Gerdjikov, I., P. Gautier, Z. Cherneva. 2006. The northwestern segment of North Rhodopian extensional system and related fabric in the Rila-Rhodopian batholith. — *National conference Geosciences, Abstracts,* (this volume)

Ivanov, Z., S. Sarov, E. Mischev, A. Vnoukovska. 1989. Le charriage des Rhodopes septentrionales entre les vallees des rivieres Čepinska et Iskar. — *Ann. Univ. Sofia, 1, Geol.,78*, 64—73.

Ivanov, Z., D. Dimov, S. Dobrev, B. Kolkovski, S. Sarov. 2000. Structure, Alpine evolution and mineralizations of the Central Rhodopes area (South Bulgaria). — *Guide to Excursion B, ABCD-GEODE 2000 Workshop, Borovets, Bulgaria*, 50 pp.

Kamenov, B., I. Peytcheva, L. Klain, K. Arsova, Y. Kostitsin, E. Salnikova. 1999. Rila-West Rhodope Batholith: Petrological and geochemical constraints for its composite character. — *Geochem., Mineral., Petrol., 36*, 3—27.

Ludwig, K. 2005. Isoplot/Ex. V. 3. USGS Open-File rep.

Ovtcharova, M., Z. Cherneva, A. von Quadt, I. Peytcheva. 2002. Migmatitic geochronology and geochemistry — a key to understanding the exhumation of the Madan dome (Bulgaria). — *12 Ann. Goldschmidt Conf. Abstracts*, Davos, Switzerland, A573.

Peytcheva, I., Y. Kostitsin, E. Salnikova, B. Kamenov, L. Klain. 1998. Rb-Sr and U-Pb isotope data for the Rila-Rhodopes batholith. — *Geochem., Mineral., Petrol., 35*, 93—105.

Todt, W., R. A. Cliff, A. Hanser, A. W. Hofmann. 1996. Evaluation of a ^{202}Pb-^{205}Pb double spike for high-precision lead isotope analysis. In: Basu, A., S. Hart (Eds.). *Earth Processes: Reading the Isotopic Code*. Geophys. Monograph 95, Am. Geophys. Union, 429—437.

Valkov, V., N. Antova, K. Dončeva. 1989. The granitoids in Rila-West Rhodope batholith. — *Geologica Balc., 19*, 2, 21—54.

von Quadt, A., I. Peycheva. 2005. The Southern extension of the Srednogorie Type Cretaceous Magmatism in Rila-Western Rhodope: Constraints from Isotope-Geochronological and geochemical Data. — *Proceedings of the Jubilee International Conference "80 years BGS"*, 113—116.

„Бебе-гранити“ в мигматити от долината на р. Чепинска, Западни Родопи — геохимия и U-Pb изотопно датиране на монацит и циркон

Златка Чернева, Мария Овчарова, Димо Димов, Албрехт фон Квадт

Резюме. Представени са първи геохроноложки и геохимични данни за мигматити от Западните Родопи, продукт на водонаситено топене в амфиболитов фациес, с образуване на малки тела от анатектичен гранит в края на регионалната пластична деформация. U-Pb изотопно датиране на циркон и монацит от тези тела характеризира възрастта на циркона унаследен отмагмен протолит с корово-мантиен произход (150 Ma), и смесени възрастови компоненти при монацита (59—63 Ma), отчасти свързани с кристализацията на анатектичната топилка.